Neuron
Article

Deletion of *Mecp2* in *Sim1*-Expressing Neurons Reveals a Critical Role for MeCP2 in Feeding Behavior, Aggression, and the Response to Stress

Sharyl L. Fyffe,[1] Jeff L. Neul,[3] Rodney C. Samaco,[1] Hsiao-Tuan Chao,[2] Shay Ben-Shachar,[1] Paolo Moretti,[1,4] Bryan E. McGill,[2] Evan H. Goulding,[6] Elinor Sullivan,[6] Laurence H. Tecott,[6] and Huda Y. Zoghbi[1,2,3,4,5,*]
[1]Department of Molecular and Human Genetics
[2]Department of Neuroscience
[3]Department of Pediatrics
[4]Department of Neurology
[5]Howard Hughes Medical Institute
Baylor College of Medicine, Houston, TX 77030, USA
[6]Department of Psychiatry, Center for Neurobiology and Psychiatry, University of California, San Francisco, San Francisco, CA 94158, USA
*Correspondence: hzoghbi@bcm.tmc.edu
DOI 10.1016/j.neuron.2008.07.030

SUMMARY

Rett Syndrome (RTT) is an autism spectrum disorder caused by mutations in the X-linked gene encoding methyl-CpG binding protein 2 (MeCP2). In order to map the neuroanatomic origins of the complex neuropsychiatric behaviors observed in patients with RTT and to uncover endogenous functions of MeCP2 in the hypothalamus, we removed *Mecp2* from *Sim1*-expressing neurons in the hypothalamus using Cre-*loxP* technology. Loss of MeCP2 in *Sim1*-expressing neurons resulted in mice that recapitulated the abnormal physiological stress response that is seen upon MeCP2 dysfunction in the entire brain. Surprisingly, we also uncovered a role for MeCP2 in the regulation of social and feeding behaviors since the *Mecp2* conditional knockout (CKO) mice were aggressive, hyperphagic, and obese. This study demonstrates that deleting *Mecp2* in a defined brain region is an excellent approach to map the neuronal origins of complex behaviors and provides new insight about the function of MeCP2 in specific neurons.

INTRODUCTION

Rett Syndrome (RTT) is a devastating X-linked neurodevelopmental disorder that affects ~1 in 10,000 females (Moretti and Zoghbi, 2006). Patients with classic RTT suffer from a broad array of phenotypes that affect almost every part of the central and autonomic nervous systems (Glaze, 2005; Weaving et al., 2005). These phenotypes include impaired social behavior and communication skills, motor abnormalities, and the development of stereotyped movements (Hagberg, 2002).

The majority (>95%) of RTT cases are caused by mutations in the gene encoding methyl-CpG-binding protein 2 (MeCP2), a protein widely expressed throughout the brain (Williamson and Christodoulou, 2006; Zoghbi, 2005). In addition to classic RTT, patients with *MECP2* mutations manifest a variety of neuropsychiatric conditions, including autism, juvenile onset schizophrenia, and bipolar disease, with mental retardation depending on the type of mutation or the pattern of X chromosome inactivation (XCI) (Cohen et al., 2002; Weaving et al., 2003). Girls typically have features of classic RTT when they have random XCI, whereby half of their cells express a mutant *MECP2* allele (Shahbazian et al., 2002b; Takagi, 2001). In contrast, patients with skewed patterns of XCI favoring the wild-type (WT) allele might display only a few features, such as autism, tremor, or other neurobehavioral deficits. Because the majority of cells in girls with favorable XCI patterns express the WT allele, the isolated phenotypes might result from loss of MeCP2 function in particular brain regions.

The creation of several mouse models carrying different *Mecp2* mutations enabled the recapitulation of many of the phenotypes seen in patients and has enhanced our appreciation of the breadth of clinical phenotypes that are associated with RTT. *Mecp2* null mice display tremor, breathing dysfunction, and hind-limb clasping; are overweight (on a mixed 129, C57BL/6, BALB/c genetic background); and die by 10 weeks (Chen et al., 2001; Guy et al., 2001). Mice bearing a truncated *Mecp2* allele ($Mecp2^{308/Y}$) are overweight (on a 129 Sv/Ev background, unpublished data); display motor dysfunction, seizures, stereotypies, altered social behavior, abnormal stress responses, and anxiety-like behavior; and die by 15 months of age (McGill et al., 2006; Moretti et al., 2005; Shahbazian et al., 2002a). Conditional deletion of *Mecp2* from neurons that express *CaMKII*-Cre93 throughout the forebrain and midbrain reproduces a large subset of RTT features, including abnormal motor coordination, anxiety-like behavior, impaired learning and memory, and weight gain (Gemelli et al., 2006). The overweight phenotype seen in each of the mouse models was initially perplexing given that girls with classic RTT are typically thin and often suffer from growth failure predominantly because of feeding difficulties due to oropharyngeal dysmotility (difficulty chewing and swallowing) (Motil et al., 1999). However, upon reflection on the clinical course of many patients with *MECP2* mutations

who do not display classic RTT, we noticed that males with hypomorphic *MECP2* mutations and females with milder variants of RTT often become obese (Couvert et al., 2001; Kleefstra et al., 2002; Zappella et al., 2001).

Studying patients with RTT, as well as mouse models of RTT, is a daunting task given the incredible range of phenotypes that stem from MeCP2 dysfunction in all neurons. Moreover, it is very difficult to dissociate phenotypes attributable to dysfunction of MeCP2 from secondary compensatory changes. Given the clinical observation that different patterns of XCI likely result in the manifestation of distinct subsets of RTT phenotypes, we proposed that particular RTT phenotypes result from loss of function of MeCP2 in specific neurons and that deleting *Mecp2* from small groups of neurons in the mouse will enable us to map specific neurobehavioral phenotypes to discrete brain regions or cell types. Furthermore, we reasoned that this strategy should allow us to uncover endogenous functions of MeCP2 that might otherwise be masked in the constitutive *Mecp2* null mice that display many phenotypes.

In this work, we focus on the hypothalamus because patients with *MECP2* mutations display many phenotypes suggestive of hypothalamic dysfunction, such as sleep abnormalities, episodes of heightened anxiety, an abnormal physiological response to stress as measured by increased levels of cortisol in the urine, gastrointestinal dysfunction, as well as cardiac and breathing abnormalities (Axelrod et al., 2006; Motil et al., 1999, 2006; Mount et al., 2002; Young et al., 2007). In this study, we utilized mice that express Cre recombinase under the control of *Sim1* regulatory elements to delete *Mecp2* in several regions of the hypothalamus using Cre-*loxP* technology. We performed a comprehensive battery of behavioral and physiological tests on *Mecp2* conditional knockout (CKO) mice and all littermate controls to screen for the presence of both RTT-like and distinct phenotypes, and we discovered that MeCP2 plays a critical role in pathways important for mediating proper physiological responses to stress as well as both social and feeding behaviors.

RESULTS

Selective Deletion of *Mecp2* in *Sim1*-Expressing Neurons

We removed *Mecp2* from *Sim1*-expressing neurons by breeding mice carrying a *Mecp2* allele flanked by *loxP* sites ($Mecp2^{flox/+}$) (Guy et al., 2001) to *Sim1*-cre BAC transgenic mice (Balthasar et al., 2005). *Sim1* regulatory elements drive Cre expression in transgenic mice during embryonic development and after birth in the paraventricular (PVN), supraoptic (SON), and posterior (PH) hypothalamic nuclei, as well as in the nucleus of the lateral olfactory tract (NLOT) of the amygdala (Balthasar et al., 2005). A small amount of scattered Cre expression also occurs in a few other areas surrounding the hypothalamus and amygdala (Balthasar et al., 2005); however, this is very minimal compared to the robust Cre expression found in the nuclei mentioned above. Fluorescent immunohistochemistry demonstrated a clear reduction of MeCP2 in all areas where Cre is expressed, including the PVN (Figures 1A and 1B) and SON (Figures 1C and 1D) of *Mecp2* conditional knockout (*Mecp2* CKO) mice. MeCP2 levels were not altered in the suprachiasmatic nucleus (SCN), an area of the hypothalamus where the Cre is not expressed (data not shown).

Mecp2 CKO Mice Display an Increased Physiological Response to Stress

To screen for the presence of RTT-like phenotypes, we performed a comprehensive battery of behavioral tests on *Mecp2* CKO mice and all littermate controls (Table 1). Although *Mecp2* CKO mice behaved similarly to their littermates in a variety of paradigms (Figure S1 available online), they also reproduced a subset of phenotypes typically detected with MeCP2 dysfunction throughout the brain (Table 1). In light of the increased urinary cortisol excretion in patients with RTT (Motil et al., 2006) and the higher serum corticosterone in $Mecp2^{308/Y}$ mice after stress (McGill et al., 2006), we examined endocrine responses to stress in *Mecp2* CKO mice. We measured serum levels of corticosterone in *Mecp2* CKO and control mice under basal conditions and after 30 min of restraint stress. We found a significant effect of genotype under basal conditions, $F(3,28) = 5.28$, $p = 0.005$, and after stress, $F(3,27) = 8.70$, $p < 0.001$. Tukey's post hoc comparisons revealed that, under basal conditions, $Mecp2^{flox}$ and *Mecp2* CKO mice had similar corticosterone levels compared to WT mice, although their levels were higher than mice that carry only the *Sim1*-cre transgene ($p < 0.05$ for both, Figure 2A). Strikingly, after 30 min of restraint, *Mecp2* CKO mice had significantly higher corticosterone levels than all littermate controls, and they exhibited a 134% increase in serum corticosterone over WT littermates ($p < 0.01$, Figure 2A). These results indicate that, similar to patients with RTT and $Mecp2^{308/Y}$ mice, *Mecp2* CKO mice have an enhanced physiologic response to stress.

We next attempted to determine whether *Mecp2* CKO mice also exhibit increased anxiety-like behavior. In the open field, there was a significant effect of genotype for the center-to-total distance ratio, $F(3,60) = 7.58$, $p < 0.001$ (Figure 2B). Tukey's post hoc comparison revealed that *Mecp2* CKO mice explored the center of an open field significantly less than all controls, a finding consistent with enhanced anxiety-like behavior. The total distance traveled in the open field was similar among *Mecp2* CKO and WT mice, indicating that the decreased exploration of the center of the arena by *Mecp2* CKO mice was not likely the result of motor impairment (Figure 2C). It should be noted, however, that we did observe a small but significant decrease in the total distance that the *Mecp2* CKO mice traveled throughout the test when compared to mice that carry only the *Sim1*-cre allele ($p < 0.01$). To confirm that the *Mecp2* CKO mice display increased anxiety-like behavior, we performed a light-dark box assay, one of the most widely used and well-documented tests for studying anxiety-like behavior (Bourin and Hascoet, 2003). Analysis of the data by two-way analysis of variance (ANOVA) demonstrated a significant effect of genotype ($Mecp2^{flox}$ × *Sim1*-cre interaction) on both the percentage of time spent in the lit side, $F(1,60) = 4.08$, $p = 0.048$, and the number of transitions between compartments, $F(1,60) = 5.85$, $p = 0.019$. Interestingly, however, one-way ANOVA with Tukey's post hoc analysis revealed that *Mecp2* CKO mice spent a similar amount of time in the lit side of the light-dark box compared to all littermate controls (Figure 2D). Furthermore, the number of transitions between

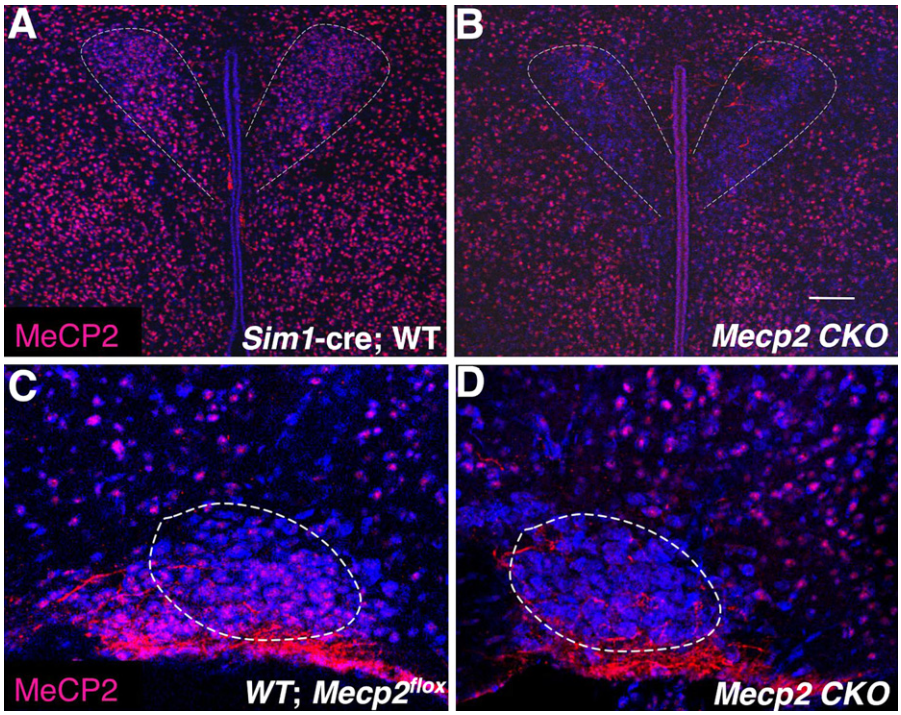

Figure 1. *Mecp2* CKO Mice Display a Decreased Amount of MeCP2 in the Paraventricular Nucleus and the Supraoptic Nucleus of the Hypothalamus Compared to Littermate Controls

Detection of MeCP2 (red) by immunofluorescence in the paraventricular nucleus (PVN) of mice carrying only the *Sim1*-cre transgene (A) and *Mecp2* CKO mice (B) and in the supraoptic nucleus (SON) of mice carrying only the *Mecp2*^{flox} allele (C) and *Mecp2* CKO mice (D). TOTO-3 staining in blue marks cell nuclei. Scale bar, 100 μm (A and B); 62.5 μm (C and D).

compartments and the latency to enter the dark were not different between *Mecp2* CKO mice and WT controls (data not shown). Thus, although *Mecp2* CKO mice clearly display an increased physiological response to stress and a decreased center-to-total distance ratio in the open field assay, the light-dark data do not reveal increased anxiety-like behavior in the *Mecp2* CKO mice.

Mecp2 CKO Mice Exhibit Abnormal Social Behavior in the Form of Increased Aggression

Mecp2 CKO mice also behaved abnormally in the partition test, which is designed to evaluate social behavior. In this test, two mice are placed in a cage divided by a clear and perforated plexiglass partition, and the amount of time that the test mouse spends near the partition investigating either a familiar or an unfamiliar partner is recorded. Repeated-measures ANOVA (genotype × time) revealed a significant effect, $F(3,59) = 10.65$, $p < 0.001$, and Tukey's post hoc analysis demonstrated that *Mecp2* CKO mice ($p < 0.001$) and mice that carry only the *Mecp2*^{flox} allele ($p < 0.05$) spent more time at the partition compared to control littermates, suggesting increased social interaction (Figure 2E). This *Mecp2*^{flox} effect is consistent with data reported in a recent study (Samaco et al., 2008). This study demonstrated that mice carrying the *Mecp2*^{flox} allele express 50% less MeCP2 compared to WT littermates, highlighting the importance of including *Mecp2*^{flox} mice as controls when interpreting data from *Mecp2* CKO experiments. Interestingly, we noticed that *Mecp2* CKO and *Mecp2*^{flox} mice engaged in very different behaviors at the partition. Mice that carry only the *Mecp2*^{flox} allele demonstrated typical social interactions, such as sniffing and exploration. In contrast, *Mecp2* CKO mice were preoccupied with aggressive behaviors, such as tail rattling directed toward the unfamiliar partner.

To further characterize these aggressive behaviors, we used the resident intruder assay. Prior to testing the response of a resident mouse to an intruder, the test mice were singly housed for 2 weeks, a procedure believed to enhance territoriality. On the test day, we recorded aggressive behaviors after placing a smaller, unfamiliar, group-housed WT mouse into the home cage of the test mouse. Scores used to denote aggressive behaviors included the number of attacks, mounting, biting, and tail rattling events. *Mecp2* CKO mice engaged in significantly more tail rattles ($p < 0.01$) and aggressive attacks ($p < 0.01$) than their control littermates (Figure 2F and Movies S1 and S2). In fact, out of the 24 control littermates tested, not a single tail rattle or attack was recorded during the test period. Notably, the aggression observed in *Mecp2* CKO mice appears to be limited to situations when they are stressed, either as a result of being singly housed or as a specific reaction to novel intruders of their territory, since they do not attack their familiar cage mates. Furthermore, they are not aggressive toward the examiner when they are handled.

Table 1. A Summary of the Behavioral Assays and Their Outcome in *Mecp2* CKO Mice

Behavior Assay	Phenotype Tested	Phenotype Observed in *Mecp2* CKO
General health exam	Body weight, stereotypies, kyphosis	Yes
Wire hang and dowel	Motor coordination	No
Tremor monitoring	Tremor	No
Light-dark box	Anxiety-like behavior	No
Open field	Anxiety-like behavior	Yes
Conditioned fear	Learning and memory	No
Partition test	Social behavior	Yes
Resident intruder	Aggression	Yes
Aging of animals	Reduced survival	No

A comprehensive battery of behavioral assays was performed on F_1 129/FVB male *Mecp2* CKO mice and their control littermates (n = 15–17/genotype) to assess whether any RTT-like features were recapitulated after deleting *Mecp2* from *Sim1*-expressing neurons.

Mecp2 CKO Mice Have Increased Body Weight, Fat Mass, and Body Length

Mecp2 CKO mice fed regular mouse chow *ad libitum* exhibited significantly increased body weight after 7 weeks of age (repeated-measures two-way ANOVA [$Mecp2^{flox}$ × *Sim1*-cre], lower-bound $F(1,60) = 19.59$, $p < 0.001$, Tukey's post hoc $p < 0.01$; Figures 3A and 3B). *Mecp2* CKO mice weigh 27% more than their control littermates by 18 weeks and 48% more by 42 weeks (Figures 3B and S2). We examined linear growth and found that *Mecp2* CKO mice also exhibit a small (3%) but significant ($p < 0.05$) increase in body length compared to littermate controls at 42 weeks of age (data not shown).

To determine whether the observed weight gain was due to increased adiposity, we dissected and weighed intra-abdominal gonadal fat pads. We found a significant effect of genotype, $F(3,28) = 8.91$, $p < 0.001$, and Tukey's post hoc comparison revealed that gonadal fat pad masses were greatly increased in the *Mecp2* CKO mice compared to all controls ($p < 0.01$, Figure 3C), suggesting that their increased body weight is primarily due to an increase in body fat deposition. In order to confirm these findings, we performed dual energy X-ray absorptiometry (DEXA) scans on *Mecp2* CKO mice to determine body composition. DEXA analysis indicated that *Mecp2* CKO mice had increased total body fat percentages (36% ± 3%) compared to control littermates (20% ± 1%) at 20 weeks of age ($p < 0.05$, Figure 3D). These data demonstrate that the increased body weight in *Mecp2* CKO mice is primarily due to increased body fat.

Mecp2 CKO Mice Display Normal Activity and Basal Metabolic Rates but Are Hyperphagic

To probe the cause of obesity in the *Mecp2* CKO mice, we used an automated home cage monitoring system to evaluate daily activity and food intake. Average daily total movement values were not significantly different between *Mecp2* CKO mice and control littermates, although a trend toward hypoactivity ($p = 0.066$) was noted in the *Mecp2* CKO mice (Figure 4A). Interestingly, on experimental day 1, *Mecp2* CKO mice completely lacked the novelty-induced hyperactivity response that is normally seen in WT mice (Figure 4A), likely due to heightened anxiety. We evaluated oxygen consumption using indirect calorimetry and found that *Mecp2* CKO mice have normal basal metabolic rates (Figure 4B). Together, these data suggest that the marked obesity observed in the *Mecp2* CKO mice is not secondary to a decrease in energy expenditure. We next evaluated energy consumption by monitoring daily food intake. After a 4 day acclimation period, we analyzed food consumption over a subsequent 4 day period. We found a significant effect of genotype, $F(3,26) = 13.17$, $p < 0.001$, and Tukey's post hoc comparison revealed that *Mecp2* CKO mice are hyperphagic, consuming, on average, 42% more chow than WT controls ($p < 0.001$, Figure 4C). Interestingly, *Mecp2* CKO mice did not consume extra chow compared to WT mice throughout the 24 hr period (experimental day 1) immediately after they were singly housed in novel cages, suggesting that they experienced stress-induced suppression of food intake during that period (Figure 4C).

Mecp2 CKO Mice Have High Serum Levels of Leptin

Feeding behavior is regulated by several signaling molecules and hormones (for a recent review, see Oswal and Yeo, 2007). One major signal that the body uses to sense energy balance is leptin, a soluble hormone secreted by adipocytes to communicate body fat deposition information to the brain. To investigate possible mechanisms responsible for mediating the hyperphagia in *Mecp2* CKO mice, we measured serum leptin levels. We did not detect any significant difference in serum leptin at 6 weeks of age, but, by 42 weeks, we found a significant effect of genotype, $F(2,17) = 31.48$, $p < 0.001$, and Tukey's post hoc comparison revealed that *Mecp2* CKO mice had a 4-fold increase ($p < 0.001$) in leptin compared to WT controls (Figure 4D). The observation that *Mecp2* CKO mice are obese in the context of elevated leptin suggests that they are able to produce and secrete leptin but are insensitive to its effects. Furthermore, because leptin levels are normal at 6 weeks, prior to the onset of obesity, we conclude that the increased leptin levels likely result from increased fat deposition in the older mice and are not due to direct leptin regulation by MeCP2.

Mecp2 CKO Mice Express High Levels of *Npy* in the Dorsomedial Nucleus of the Hypothalamus (DMH)

Since the melanocortin pathway is an important mediator of leptin signaling in the hypothalamus (Oswal and Yeo, 2007), we next evaluated the expression of several members of this pathway, including the melanocortin 4 receptor (*Mc4r*), pro-opiomelanocortin (*Pomc1*), agouti-related protein (*Agrp*), and neuropeptide Y (*Npy*), by in situ hybridization in *Mecp2* CKO mice and control littermates. POMC and AgRP/NPY neurons in the arcuate nucleus (ARC) are activated and repressed by leptin, respectively, and they project to the PVN where POMC neurons stimulate and AgRP/NPY neurons block the activity of MC4Rs (Haskell-Luevano and Monck, 2001; Schwartz et al., 1997). Proper MC4R signaling in the PVN is critical for the regulation of food intake (Balthasar et al., 2005). RNA in situ hybridization revealed that expression of *Mc4r* in the PVN (Figures 5A and 5B) and *Pomc1* (Figures 5C and 5D) and *Agrp* in the ARC (Figures 5E

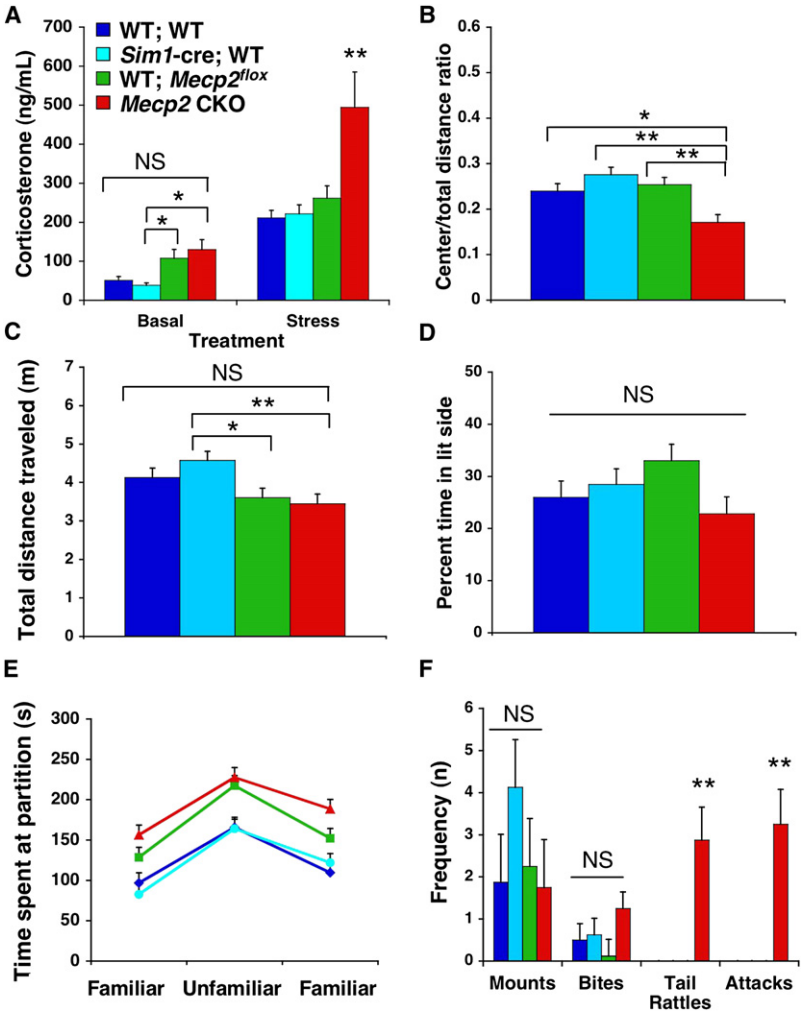

Figure 2. Deletion of *Mecp2* from *Sim1*-Expressing Neurons Results in an Abnormal Stress Response, Decreased Movement in the Center of an Open Field Arena, and Aggressive Behaviors

(A) Serum corticosterone measurement by enzyme-linked immunosorbent assay (ELISA) before and after 30 min of stress in *Mecp2* CKO mice and control littermates (n = 7–9/genotype). Under basal conditions, WT;*Mecp2*^{flox} and *Mecp2* CKO mice had higher serum corticosterone levels compared to *Sim1*-cre;WT mice; however, there was no significant difference between WT and *Mecp2* CKO mice. After stress, *Mecp2* CKO mice had significantly higher serum corticosterone levels compared to all littermates.

(B) Open field analysis revealed that *Mecp2* CKO mice had a lower center-to-total distance ratio compared to all littermate controls.

(C) The total distance traveled during the open field assay was significantly less for WT;*Mecp2*^{flox} and *Mecp2* CKO mice compared to *Sim1*-cre;WT littermates. No significant differences were found between WT and *Mecp2* CKO mice.

(D) *Mecp2* CKO mice spent a similar amount of time in the lit side of the light-dark box compared to all littermate controls.

(E) Partition test for social interaction revealed that both WT;*Mecp2*^{flox} ($p < 0.05$) and *Mecp2* CKO ($p < 0.01$) mice spent significantly more time at the partition compared to their WT and *Sim1*-cre;WT littermates.

N = 15–17/genotype for (B–E).

(F) In the resident intruder assay (n = 8/genotype), *Mecp2* CKO mice exhibited significantly more tail rattles and attacks compared to all littermate controls.

The colors used to denote genotypes are consistent for all graphs. *$p < 0.05$, **$p < 0.01$, NS = nonsignificant for all panels. Error bars represent ± SEM.

and 5F) was not altered in *Mecp2* CKO mice. Quantitative reverse transcriptase PCR (QRT-PCR) using cDNA from hypothalamus confirmed that *Mc4r*, *Pomc1*, and *Agrp* mRNA levels were not significantly different between *Mecp2* CKO mice and control littermates (data not shown). In contrast, *Npy* expression was reduced in the ARC but greatly induced in the DMH of *Mecp2* CKO mice (Figures 5G and 5H). Increased expression of *Npy* in the DMH occurs in several hyperphagic models of reduced MC4R signaling, including the agouti yellow mutant (A^y), *Mc4r* −/− mice, and WT rats during lactation, suggesting that *Npy* in the DMH may be involved in feeding regulation mediated by MC4R signaling (Chen et al., 2004; Kesterson et al., 1997). The robust expression of *Npy* in the DMH of *Mecp2* CKO mice suggests that, although *Mc4r*, *Pomc1*, and *Agrp* RNA levels are all normal, MC4R signaling may be disrupted in *Mecp2* CKO mice.

The Expression of Two MC4R Downstream Targets Is Decreased in *Mecp2* CKO Mice

We next sought to determine whether any downstream components of the MC4R signaling pathway were altered in *Mecp2* CKO mice. RNA in situ hybridization revealed that *Bdnf*, a neurotrophic factor important for weight regulation (Rios et al., 2001) and proposed to function as a downstream mediator of MC4R signaling (Tsao et al., 2008; Xu et al., 2003), was significantly decreased in the PVN of *Mecp2* CKO mice compared to WT littermates (Figures 6C and 6D). In contrast, *Bdnf* expression in *Mecp2* CKO mice was comparable to littermate controls in several nuclei of the amygdala (Figures 6A and 6B) and in the ventromedial nucleus of the hypothalamus (VMH) (Figures 6E and 6F). To quantify *Bdnf* expression, the in situ images from four to seven mice per genotype were pseudocolored using the Celldetekt protocol to determine the relative expression level on a per cell basis (Carson et al., 2005), and, subsequently, the total number of *Bdnf*-expressing cells was counted throughout the PVN (Figure 6G) and the VMH (Figure 6H). We found a 50% decrease ($p < 0.05$) in the number of cells that express *Bdnf* in the PVN of *Mecp2* CKO mice (Figure 6G). The fact that *Bdnf* expression was altered only in areas of the brain where there was strong Cre expression and *Mecp2* was deleted (PVN) suggests that *Bdnf* levels are directly affected by the loss of MeCP2.

In addition to BDNF, CRH has also been suggested as a downstream mediator of MC4R signaling (Lu et al., 2003). RNA in situ hybridization revealed a significant decrease in *Crh* in the PVN of

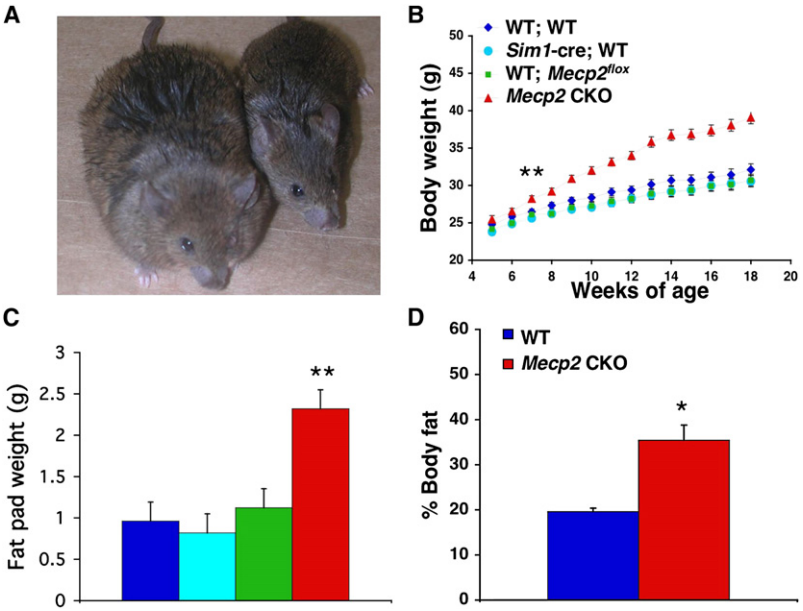

Figure 3. *Mecp2* CKO Mice Have Increased Body Weight and Body Fat

(A) *Mecp2* CKO and WT littermate at 40 weeks of age.

(B) *Mecp2* CKO mice had significantly increased body weight compared to all littermate controls beginning at 7 weeks of age (n = 15–17/genotype).

(C) *Mecp2* CKO mice had significantly increased intra-abdominal fat pad weight compared to all littermate controls (n = 8/genotype).

(D) *Mecp2* CKO mice had significantly increased percent body fat compared to WT controls as determined by DEXA scanning.

The colors used to denote genotypes are consistent for all graphs. *p < 0.05, **p < 0.01, NS = nonsignificant. Error bars represent ± SEM.

Mecp2 CKO mice (Figures 7A and 7B). Finally, overexpression of *SIM1* completely rescues the hyperphagia that occurs in A^y mice where MC4R signaling has been disrupted, suggesting that *Sim1* also acts downstream of the *Mc4r* in PVN neurons to regulate food intake (Kublaoui et al., 2006). QRT-PCR demonstrated that, in contrast to both *Bdnf* and *Crh*, the expression of *Sim1* is not altered in the *Mecp2* CKO hypothalamus (Figure S3A). To confirm that the expression of other genes that are highly expressed in the PVN was similarly unaltered in *Mecp2* CKO mice, we examined the expression of arginine vasopressin (*Avp*) and oxytocin (*Oxt*) by QRT-PCR (Figures S3B and S3C). We found that both *Avp* and *Oxt* are expressed at WT levels in the *Mecp2* CKO hypothalamus, suggesting that the cells in the PVN retain at least some of their normal function.

DISCUSSION

In this study, we demonstrate that deletion of *Mecp2* in *Sim1*-expressing neurons results in a subset of the phenotypes observed in RTT and related *MECP2* disorders. We found that *Mecp2* CKO mice recapitulated the increased body weight and abnormal stress response that are observed in mice where *Mecp2* is mutated in all neurons. This result is interesting in light of the fact that patients with RTT syndrome have also been found to exhibit an abnormal physiological response to stress (Motil et al., 2006). Importantly, we did not recapitulate all of the phenotypes typically seen upon deletion of *Mecp2* from the entire brain, such as motor coordination abnormalities and learning and memory deficits, demonstrating that the function of MeCP2 in *Sim1*-expressiong neurons is likely not important for those behaviors. By removing *Mecp2* from

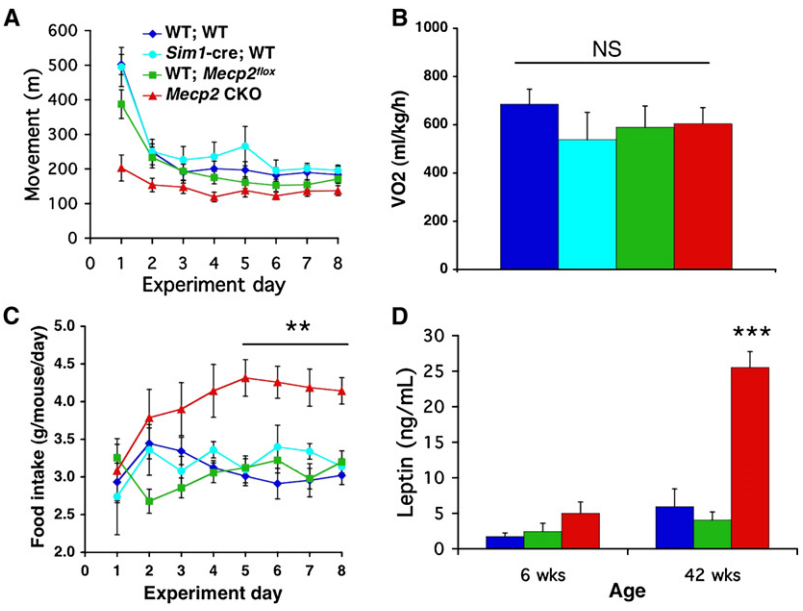

Figure 4. *Mecp2* CKO Mice Have Normal Activity Levels and Basal Metabolic Rates but Display Increased Food Intake and Serum Leptin Levels

(A) The 24 hr total movement values over 8 days. No significant differences were identified after 4 days of acclimation.

(B) Oxygen consumption values as measured by an indirect open circuit calorimeter system revealed no significant differences between genotypes.

(C) The 24 hr food intake values over 8 days. *Mecp2* CKO mice consume significantly more chow than all of their control littermates.

N = 5–9/genotype for (A–C).

(D) Serum leptin measurement by ELISA at 6 weeks (n = 4/genotype) and at 42 weeks (n = 6–7/genotype) in *Mecp2* CKO mice and control littermates. *Mecp2* CKO mice had increased serum leptin levels compared to all littermate controls at 42 weeks, but not at 6 weeks of age.

The colors used to denote genotypes are consistent for all graphs. **p < 0.01, ***p < 0.001, NS = nonsignificant. Error bars represent ± SEM.

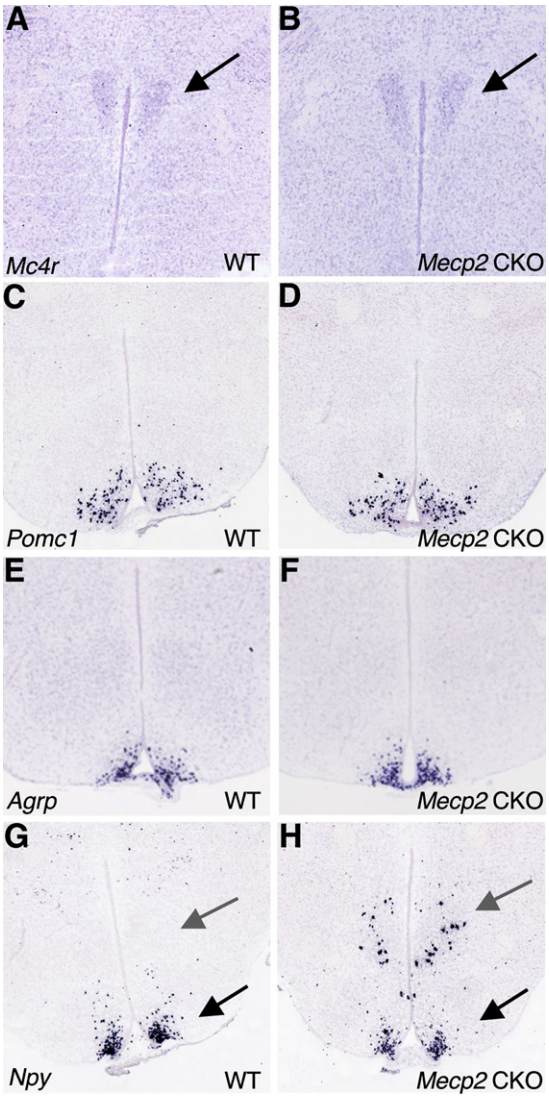

Figure 5. RNA In Situ Hybridization Demonstrates that *Mecp2* CKO Mice Have Normal Expression of *Mc4r, Pomc1,* and *Agrp* but Altered *Npy* Compared to WT Controls

(A) *Mc4r* expression in WT PVN.
(B) *Mc4r* expression in *Mecp2* CKO PVN.
(C) *Pomc1* expression in WT ARC.
(D) *Pomc1* expression in *Mecp2* CKO ARC.
(E) *Agrp* expression in WT ARC and (F) *Mecp2* CKO ARC.
(G) *Npy* expression in WT DMH (gray arrow) and ARC (black arrow).
(H) *Npy* expression is greatly increased in DMH (gray arrow) but decreased in the ARC (black arrow) of *Mecp2* CKO mice compared to WT littermates.

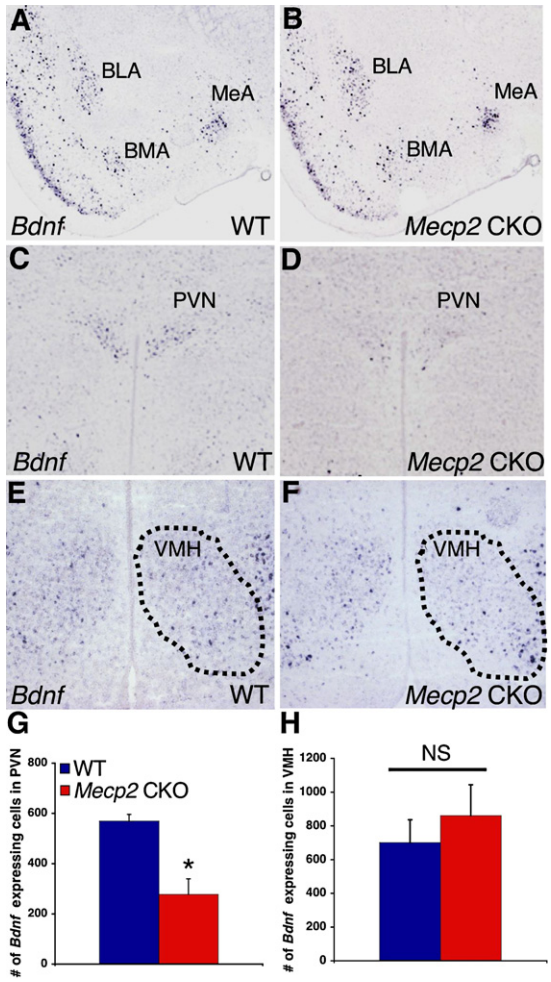

Figure 6. RNA In Situ Hybridization Demonstrates that *Mecp2* CKO Mice Display Decreased Expression of *Bdnf* in the PVN but Normal Expression throughout the Amygdala

Bdnf expression throughout the basolateral amygdala (BLA), basomedial amygdala (BMA), and the medial amygdala (MeA) in (A) WT and (B) *Mecp2* CKO mice. *Bdnf* expression in (C) WT and (D) *Mecp2* CKO PVN. *Bdnf* expression in (E) WT VMH and (F) *Mecp2* CKO VMH. The outlined area highlights the VMH. *Bdnf*-expressing neurons were counted on sections throughout the (G) PVN and (H) VMH.
Error bars represent ± SEM.

Sim1-expressing neurons, we also uncovered a role for MeCP2 in the MC4R signaling pathway that regulates food intake and in pathways important for aggression. Although aggression and hyperphagia are not typically seen in patients with classic RTT, patients with atypical RTT owing to favorable XCI or to hypomorphic *MECP2* alleles do, indeed, manifest aggressive behavior (P. Huppke, personal communication; H.Y.Z., unpublished data), and some are overweight (Couvert et al., 2001; Kleefstra et al., 2002; Zappella et al., 2001). It is possible that these phenotypes are not observed upon MeCP2 dysfunction in all neurons due to secondary changes that may mask certain primary effects of MeCP2 dysfunction. It is noteworthy that deletion of *Mecp2* from other selected brain regions, such as the Purkinje cells of the cerebellum or tyrosine hydroxylase neurons, does not result in similar phenotypes (J.L.N. and H.Y.Z., unpublished data), highlighting the specificity of the phenotypes observed in this study and the important role of *Mecp2* in the hypothalamus.

Mecp2 CKO mice displayed increased aggressive behavior that was apparent strictly upon changes in social situations, such as exposure to either an unfamiliar or intruder mouse. The fact that aggression is not detected in the home cage but

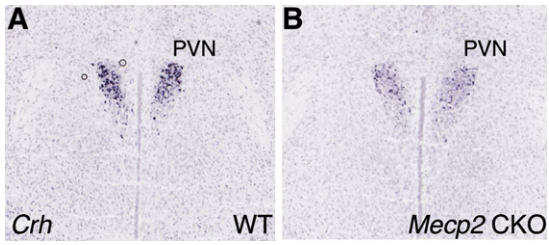

Figure 7. RNA In Situ Hybridization Demonstrates that *Mecp2* CKO Mice Display Decreased Expression of *Crh* in the PVN
Crh expression in representative sections of (A) WT and (B) *Mecp2* CKO PVN.

is precipitated by the stress of unfamiliarity is interesting given that patients with autism spectrum disorders typically manifest aggression when stressed or frustrated. When interpreting the resident intruder data, it is of note that the *Mecp2* CKO mice were heavier than their control littermates. The intruder mice were slightly smaller than all of the mice that were tested, although this difference in body weight was more pronounced in the case of the *Mecp2* CKO mice because the latter are much larger than their control littermates. While it is possible that the increased body weight of the *Mecp2* CKO mice may have contributed to the development of their increased aggression, the fact that the aggressive behavior was detected only in response to a smaller novel mouse and not in response to their smaller regular cage mates suggests that the increased body weight alone is not likely responsible for the aggressive phenotype.

Stress undoubtedly represents an altered physiological state; thus, the finding that *Mecp2* CKO mice cannot easily adjust to a new state adds to the growing evidence suggesting that MeCP2 is important for the modulation of gene expression in response to alterations in neuronal activity owing to new physiologic states (Chahrour and Zoghbi, 2007; Chen et al., 2003). For example, MeCP2 is important for the neuronal activity-dependent regulation of *Bdnf* (Zhou et al., 2006). Furthermore, genes that are normally induced in response to stress, such as serum glucocorticoid-inducible kinase 1 (*Sgk1*) and FK506-binding protein 5 (*Fkbp5*), are misregulated in the *Mecp2* null brain (Nuber et al., 2005). Although we do not yet understand the molecular basis for the aggression phenotype seen in the *Mecp2* CKO mice, we have demonstrated that MeCP2's function, specifically in *Sim1*-expressing neurons, is critical to ensure proper social behavior in response to novel and stressful social situations.

We also found that *Mecp2* CKO mice are obese based on their significantly increased body weight, close to a 100% increase in body fat content by 20 weeks of age, and an apparent resistance to leptin. *Mecp2* CKO mice display normal levels of activity and basal metabolic rates, but they consume more chow than control littermates. Once again, deletion of *Mecp2* in *Sim1*-expressing neurons impairs the ability of the mouse to adapt to changing physiology; in this case, *Mecp2* CKO mice do not stop eating once they have ingested a sufficient number of calories, demonstrating that they are unable to properly respond to satiety signals.

Hyperphagia and obesity are characteristic of mice that have disrupted MC4R signaling. MC4Rs function by integrating an agonist satiety signal from α-MSH (a cleavage product of POMC) and an antagonist signal provided by AgRP (Oswal and Yeo, 2007). The essential role of MC4Rs in the control of food intake is evident based on the hyperphagia and severe obesity seen in *Mc4r* −/− mice (Huszar et al., 1997), mice that overexpress the MC4R antagonist (A^y) (Kesterson et al., 1997), and in humans with naturally occurring mutations in *MC4R* (Lubrano-Berthelier et al., 2006). MC4Rs are densely expressed in the PVN, an area that receives inputs from both POMC and AgRP/NPY neurons, and their function, specifically in the PVN, is essential to maintain proper control of food intake (Balthasar et al., 2005). We demonstrate that *Mecp2* CKO mice express normal levels of *Mc4r*, *Pomc1*, and *Agrp*, but they have a small decrease in *Npy* in the ARC and a profound induction of *Npy* in the DMH. The finding that *Npy* is decreased in the ARC is not surprising since NPY neurons in the ARC typically respond to increases in leptin by downregulating the expression of *Npy* (Stephens et al., 1995). Increased *Npy* expression in the DMH, however, has been noted in a variety of rodent models that exhibit reduced function of melanocortin pathways, including the agouti yellow mice (A^y), *tubby* mice, diet-induced obese mice (DIO), *Mc4r* −/− mice, and WT lactating rats (Chen et al., 2004; Guan et al., 1998; Kesterson et al., 1997). Importantly, increased expression of *Npy* in the DMH is not associated with all models of genetic obesity since leptin-deficient *ob/ob* mice do not display detectable levels of *Npy* in the DMH (Kesterson et al., 1997). Thus, the ectopic expression of *Npy* in the DMH serves as a marker of disrupted MC4R signaling, which seems to be occurring in the *Mecp2* CKO mice.

Because our data point to a disruption of MC4R signaling in the *Mecp2* CKO mice despite normal expression of upstream components of the pathway, we examined some of the downstream mediators of MC4R signaling in the PVN. Recent studies have suggested that both CRH and BDNF function as downstream effectors in the MC4R signaling pathway (Lu et al., 2003; Tsao et al., 2008; Xu et al., 2003). We found decreased expression of *Crh* in the PVN of the *Mecp2* CKO mice. This is interesting because MC4R agonists increase the expression of *Crh* in the PVN (Lu et al., 2003), whereas *Mc4r* −/− mice have low levels of *Crh* in the PVN (see discussion in Lu et al., 2003), suggesting that the decreased *Crh* observed in the *Mecp2* CKO mice may represent another marker of disrupted MC4R signaling.

We also found that *Bdnf* expression was decreased strictly in the PVN of *Mecp2* CKO mice. Studies in neuronal cultures suggest that *Bdnf* is a direct target of MeCP2 and that MeCP2 functions as a transcriptional repressor to inhibit *Bdnf* transcription specifically from promoter III (Chen et al., 2003; Martinowich et al., 2003). These data conflict, however, with recent in vivo evidence demonstrating that BDNF levels are low rather than high in *Mecp2* null mouse brain (Chang et al., 2006). Our data showing that *Bdnf* is decreased in neurons lacking MeCP2 is consistent with the in vivo data. Because low levels of *Bdnf* occur only in the cells where *Mecp2* has been deleted in the *Mecp2* CKO mice, it seems likely that the decreased expression is occurring as a primary result of MeCP2 deficiency. Given recent data showing that MeCP2 binds to the promoter region of many actively expressed genes (Yasui et al., 2007), that MeCP2 can function as both an activator and a repressor of gene expression in the hypothalamus (Chahrour et al., 2008), that *Bdnf* is

significantly downregulated in *Mecp2* null mice, and that MeCP2 overexpression results in increased *BDNF* III transcript levels in cultured rat neurons and in *MECP2* transgenic mice (Chahrour et al., 2008; Chang et al., 2006; Klein et al., 2007), we propose that MeCP2 functions as an activator of *Bdnf* transcription.

Several studies have documented the importance of BDNF in the VMH and DMH for feeding regulation (Tsao et al., 2008; Unger et al., 2007; Xu et al., 2003). A^y obese mice that have disrupted MC4R signaling have a 30%–40% decrease in *Bdnf* expression in the VMH, but no changes were observed in the PVN, DMH, or lateral hypothalamus (LH) (Xu et al., 2003). Our data suggest a disruption in MC4R signaling, although we see decreased *Bdnf* expression in the PVN and not the VMH. This result is not surprising since we have only deleted *Mecp2* from the PVN, not the VMH, and we believe that the misregulation of *Bdnf* is occurring as a direct result of the absence of MeCP2. Future studies should examine *Bdnf* expression in the VMH and the PVN of *Mc4r* −/− mice to determine whether decreased expression occurs in one or both nuclei. Data supporting the fact that BDNF is important specifically in the PVN has come from a recent study that demonstrated that BDNF administration into the PVN was sufficient to significantly decrease food intake and body weight in mice (Wang et al., 2007). MC4Rs are densely expressed in the PVN, and activation of these receptors leads to an acute release of BDNF in the hypothalamus, which is necessary for MC4R-induced effects on appetite (Nicholson et al., 2007). If MeCP2 is important for the activation of *Bdnf* transcription, then the required release of BDNF in response to MC4R activation would likely be impaired, at least in the PVN of *Mecp2* CKO mice.

We have demonstrated that MeCP2 plays an important role in the hypothalamus, an area of the brain where neurons are constantly responding to a variety of physiological stimuli. Specifically, we have demonstrated that the loss of MeCP2 seems to disrupt the typical homeostatic responses to food intake, novel environment, and stress, consistent with a role for MeCP2 in the modulation of neuronal responses to changing stimuli (Chahrour and Zoghbi, 2007; Chen et al., 2003; Zhou et al., 2006). It is interesting that we found decreased expression of *Bdnf* in the PVN of *Mecp2* CKO mice since conditional deletion of *Bdnf* from postmitotic neurons results in enhanced aggression and obesity (Koizumi et al., 2006; Lyons et al., 1999; Rios et al., 2001). Therefore, our data support a model where MeCP2 is required for the proper expression of *Bdnf* in the PVN, and we propose that misregulation of *Bdnf* expression may lead to disrupted social behavior in the form of aggression and to hyperphagia and obesity, owing to disrupted MC4R signaling.

Importantly, by using a conditional knockout strategy, we were able to reproduce a subset of RTT or *Mecp2* null phenotypes and uncover additional functions of MeCP2. The many phenotypes that are seen in patients with RTT stem from MeCP2 dysfunction in neurons throughout the brain. Our study suggests that conditional deletion of *Mecp2* in different cell populations or different regions of the brain will enable us to map the neuroanatomic origins of the complex behaviors and phenotypes seen in RTT and *MECP2* disorders. Lastly, this study revealed that the more restrictive we are in choosing the neurons in which to delete *Mecp2*, the more we will learn about the function of MeCP2 in specific neurons and the neurobiological basis of certain behaviors.

EXPERIMENTAL PROCEDURES

Animals

Mice were maintained on a 12 hr light, 12 hr dark cycle with regular mouse chow and water *ad libitum*. *Mecp2*^{flox} mice were a gift from Adrian Bird, and *Sim1*-cre mice were from Brad Lowell and Joel Elmquist. All of the mice used in these experiments were generated by crossing heterozygous female *Mecp2*$^{flox/+}$ mice that had been backcrossed to 129 Sv/Ev for seven generations to male *Sim1*-cre mice on a pure FVB background. F_1 129/FVB male littermates (64) representing all four possible genotypes were group-housed immediately after weaning so that each cage contained one mouse of each genotype. All research and animal care procedures were approved by the Baylor College of Medicine Animal Care and Use Committee.

MeCP2 Immunostaining

Mice were anesthetized (avertin) and perfused with 10% formalin for 8 min. Brains were dissected and postfixed in 10% formalin overnight at 4°C. The samples were cryoprotected in 30% sucrose/1 × PBS, and 50 μm sections were cut from hypothalamus blocks and suspended in 24-well tissue culture plates containing 1 × PBS. Sections were blocked in 2% normal goat sera with 0.3% Triton X-100 for 1 hr at 4°C, incubated for 48 hr in a 1:100 dilution of anti-MeCP2 (Upstate cat. no. 07-013), and then incubated for 48 hr in 1:500 Cy3-labeled goat-anti-rabbit (Jackson ImmunoResearch Labs). 1:2000 TOTO-3 (Invitrogen cat. no. T3604) was added to the last wash. Sections were mounted with ProLong Gold antifade mounting medium (Invitrogen cat. no. P-36931). Images were collected from optical sections that were obtained using a Zeiss 510 confocal microscope and processed using ImageJ (http://rsb.info.nih.gov/ij/).

Corticosterone Measurement

Mice were left undisturbed for 12 hr and then retro-orbitally bled between 07:00 and 09:00 hr. Before the first bleed, half of the animals were restrained in 50 ml conical tubes for 30 min (stress condition). The remaining animals were kept in their home cages (basal condition). At 3 weeks later, the mice were bled again, this time with the conditions reversed. Blood was collected in prechilled tubes containing lithium heparin and centrifuged at 0.8 × g for 10 min, and serum was collected and frozen at −80°C until it was analyzed. Serum corticosterone levels were measured using an enzyme-linked immunosorbent assay (ELISA) (IDS Inc., Fountain Hills, AZ). The data were analyzed by one-way ANOVA with Tukey's post hoc analysis.

Behavioral Assays

Open Field Assay

The experiment was performed as previously described (Spencer et al., 2006) with a few modifications. The open field apparatus consisted of a clear, open-topped Plexiglas box (40 × 40 × 30 cm) with photo beams to record the movement of the mouse within the box. Overhead lighting provided 200 lux of illumination and a white noise generator (Lafayette Instruments, Lafayette, IN) maintained background noise at 60 dB. Mice at 15 weeks of age were placed in the center of the box, and their activity was quantified over a 30 min period. Data were collected by a computer-operated digiscan optical animal activity system (Acuscan Electronics, Columbus, OH). Data were analyzed by one-way ANOVA with Tukey's post hoc analysis.

Light-Dark Box

The assay was performed as described (Spencer et al., 2006) with a few modifications. The light-dark box consisted of a clear Plexiglas chamber (36 × 20 × 26 cm) with an open top separated from a covered black chamber (15.5 × 20 × 26 cm) by a black partition with a small opening. The open chamber was illuminated to 700 lux. Mice at 14 weeks of age were placed into the illuminated side and allowed to explore freely for 10 min. Mice were scored for the number and latency of entries and time spent in each compartment, using a hand-held computer (Psion Workabout mx, Psion Teklogix) with the Observer program (Noldus Information Technologies). An entry was scored when the mouse

placed all four feet into either the light or dark zone. White noise was present at 60 dB in the test chamber. Data were analyzed by two-way ANOVA for a *Mecp2*^{flox} allele × *Sim1*-cre allele interaction and by one-way ANOVA with Tukey's post hoc analysis.

Partition Test

This test was performed as previously described (Spencer et al., 2005) with a few modifications. Test mice at 20 weeks of age were individually housed in standard housing cages for 4 days. Each cage was separated into two compartments by a perforated barrier. On day 5 of individual housing, age- and gender-matched C57/BL6 partner mice were placed into the compartment opposite the test mice. Paired mice were cohoused in the separate halves of the partitioned cage for at least 18 hr. Following this period of induced familiarity, the time that test mice displayed directed interest in their partner mice was recorded during three different paradigms: test subject versus familiar partner, test subject versus unfamiliar partner, and repeated test subject versus familiar partner. Each behavioral paradigm was assessed during three 5 min intervals and was performed in sequential order. The presence or absence of aggressive behavior (direct attacks through the partition holes and tail rattling) was also scored during the three test intervals. Data were analyzed using a repeated-measures ANOVA (genotype × time) and Tukey's post hoc analysis.

Resident Intruder

Mice at 42 weeks of age were individually housed for 2 weeks prior to the test to establish dominance in their home cage. Each singly housed test male was confronted with a lighter, group-housed WT opponent (C57BL/6) in its home cage for 10 min. The occurrence of mounting, biting, tail rattling, and attacking was recorded. To avoid injuries, the experiment was stopped if intense fighting occurred. Data were analyzed by a nonparametric Kruskal-Wallis test.

Home Cage Behavioral Monitoring and Food Intake Measurements

Food and water intake measurements were performed similarly to what was described in Wade et al. (2008) with a few modifications. Mice were individually housed for 8 days in cages (45 × 24 × 17 cm) with feeders and water bottles mounted at one end. Intake of food and water were determined daily. The cages were placed on activity-monitoring platforms with two load beams at the front of the platform and a central pivot that allowed estimation of the position of the animal's center of gravity (DiLog Instruments, Tallahassee, FL). Data were collected from the activity platform into daily event files using two personal computers (DiLog Instruments, Tallahassee, FL). A movement event was defined as the detection of a change in the animal's center of gravity beyond a radius of 1 cm (calculated online from the animal's body weight and the forces on two load beams after filtering with a 500 ms moving average window). The movement event files recorded the onset of movement events sampled every 20 ms as well as the distance moved in x and y. The amount of food consumed was measured by weighing the chow placed in the cage each morning and subtracting the amount of chow left after a 24 hr period. Mean food intake and movement for the last 4 days of data collection was used for group comparisons to allow 4 days of acclimation to the housing conditions. Data were analyzed by one-way ANOVA with Tukey's post hoc analysis.

Basal Metabolic Rate Determination

Indirect calorimetry was performed to determine oxygen consumption. Mice were placed in a four-chamber indirect open circuit calorimeter system (Oxymax; Columbus Instruments, Columbus, OH) maintained at 22°C. Food was removed at 12:00 hr. The mice were placed in the calorimetry chamber at 13:00 hr and were removed from the system at 18:00 hr. Each chamber (dimensions: 20 × 10 × 12 cm) received an airflow rate of 600 ml/min, and samples were collected at 15 min intervals. The calorimetry chambers were placed within photobeam activity monitors (San Diego Instruments, San Diego, CA) in order to measure physical activity simultaneously. Estimates of resting oxygen consumption or basal metabolic rate were made by averaging VO_2 measurements during periods when the mice broke ten beams or less. Data were analyzed by one-way ANOVA with Tukey's post hoc analysis.

Body Weight, Body Length, and Body Fat Measurements

Weight gain was measured each week beginning after weaning until 18 weeks of age. Nose-to-anus distance was measured after lightly anesthetizing each mouse in order to permit similar body extension. Intra-abdominal fat pads were dissected and weighed after the mice were anesthetized with isofluorane and then cervically dislocated. A Lunar PIXImus Densitometer (GE Medical Systems) was used to perform DEXA scans, and Lunar PIXImus 2.10 software was used to analyze the results in order to estimate percent body fat. The average of two scans was used for each mouse. Before the scan, mice were anesthetized using avertin at a dosage of 0.017–0.020 cc/g. Body weight data were analyzed using repeated-measures ANOVA with Tukey's post hoc, body length and fat pad weights were analyzed by one-way ANOVA with Tukey's post hoc, and percent body fat was analyzed by Student's t test.

Leptin Measurement

Blood was collected between 13:00 hr and 16:00 hr by retro-orbital bleed. Serum leptin levels were measured using a commercially prepared mouse leptin enzyme-linked immunoassay kit (American Laboratory Products Company, Windham, NH; cat. no. 22-LEP-E06, lot no. 090107). Data were analyzed by one-way ANOVA with Tukey's post hoc.

Nonradioactive In Situ Hybridization (ISH)

Coronal sections from two to four mice of each genotype were analyzed for each gene. Tissue preparation and automated ISH were performed as previously described (Carson et al., 2002; Visel et al., 2004; Yaylaoglu et al., 2005) and as described online at http://www.genepaint.org/RNA.htm. *Mc4r*, *Pomc1*, *Agrp*, *Npy*, *Bdnf*, and *Crh* antisense probes were generated from cDNA clones. The cDNA templates were amplified by PCR and used for in vitro transcription of digoxygenin-labeled riboprobe. We performed quantitative analysis of the *Bdnf* ISH signal on sections spanning the entire PVN and VMH using the Celldetekt protocol to determine cellular gene expression strengths (Carson et al., 2005). Data were analyzed using a two-tailed Student's t test.

SUPPLEMENTAL DATA

The Supplemental Data include Supplemental Experimental Procedures, three figures, and two movies and can be found with this article online at http://www.neuron.org/cgi/content/full/59/6/947/DC1/.

ACKNOWLEDGMENTS

We are grateful to B. Lowell and J. Elmquist for the gift of *Sim1*-cre mice; to A. Bird for *Mecp2*^{flox} mice; to the Baylor College of Medicine MRDDRC confocal core; to Christina Thaller and the Baylor College of Medicine in situ core; to the Emory University Biomarkers Core Lab for technical assistance; to the CNRC Body Composition Lab for DEXA scans; and to M. Ramocki and other Zoghbi lab members for helpful comments on the manuscript. This work was funded by National Institutes of Health/National Institute of Neurological Disorders and Stroke grant NS057819 (H.Y.Z.), National Institute of Child Health and Human Development Mental Retardation and Developmental Disabilities Research Center HD024064 (H.Y.Z.), the International Rett Syndrome Foundation, Autism Speaks (R.C.S.), and the Simons Foundation. H.Y.Z. is a Howard Hughes Medical Institute investigator.

Accepted: July 21, 2008
Published: September 24, 2008

REFERENCES

Axelrod, F.B., Chelimsky, G.G., and Weese-Mayer, D.E. (2006). Pediatric autonomic disorders. Pediatrics *118*, 309–321.

Balthasar, N., Dalgaard, L.T., Lee, C.E., Yu, J., Funahashi, H., Williams, T., Ferreira, M., Tang, V., McGovern, R.A., Kenny, C.D., et al. (2005). Divergence of melanocortin pathways in the control of food intake and energy expenditure. Cell *123*, 493–505.

Bourin, M., and Hascoet, M. (2003). The mouse light/dark box test. Eur. J. Pharmacol. *463*, 55–65.

Carson, J.P., Thaller, C., and Eichele, G. (2002). A transcriptome atlas of the mouse brain at cellular resolution. Curr. Opin. Neurobiol. *12*, 562–565.

Carson, J.P., Eichele, G., and Chiu, W. (2005). A method for automated detection of gene expression required for the establishment of a digital transcriptome-wide gene expression atlas. J. Microsc. *217*, 275–281.

Chahrour, M., and Zoghbi, H.Y. (2007). The story of Rett syndrome: from clinic to neurobiology. Neuron *56*, 422–437.

Chahrour, M., Jung, S.Y., Shaw, C., Zhou, X., Wong, S.T., Qin, J., and Zoghbi, H.Y. (2008). MeCP2, a key contributor to neurological disease, activates and represses transcription. Science *320*, 1224–1229.

Chang, Q., Khare, G., Dani, V., Nelson, S., and Jaenisch, R. (2006). The disease progression of Mecp2 mutant mice is affected by the level of BDNF expression. Neuron *49*, 341–348.

Chen, R.Z., Akbarian, S., Tudor, M., and Jaenisch, R. (2001). Deficiency of methyl-CpG binding protein-2 in CNS neurons results in a Rett-like phenotype in mice. Nat. Genet. *27*, 327–331.

Chen, W.G., Chang, Q., Lin, Y., Meissner, A., West, A.E., Griffith, E.C., Jaenisch, R., and Greenberg, M.E. (2003). Derepression of BDNF transcription involves calcium-dependent phosphorylation of MeCP2. Science *302*, 885–889.

Chen, P., Williams, S.M., Grove, K.L., and Smith, M.S. (2004). Melanocortin 4 receptor-mediated hyperphagia and activation of neuropeptide Y expression in the dorsomedial hypothalamus during lactation. J. Neurosci. *24*, 5091–5100.

Cohen, D., Lazar, G., Couvert, P., Desportes, V., Lippe, D., Mazet, P., and Heron, D. (2002). MECP2 mutation in a boy with language disorder and schizophrenia. Am. J. Psychiatry *159*, 148–149.

Couvert, P., Bienvenu, T., Aquaviva, C., Poirier, K., Moraine, C., Gendrot, C., Verloes, A., Andres, C., Le Fevre, A.C., Souville, I., et al. (2001). MECP2 is highly mutated in X-linked mental retardation. Hum. Mol. Genet. *10*, 941–946.

Gemelli, T., Berton, O., Nelson, E.D., Perrotti, L.I., Jaenisch, R., and Monteggia, L.M. (2006). Postnatal loss of methyl-CpG binding protein 2 in the forebrain is sufficient to mediate behavioral aspects of Rett syndrome in mice. Biol. Psychiatry *59*, 468–476.

Glaze, D.G. (2005). Neurophysiology of Rett syndrome. J. Child Neurol. *20*, 740–746.

Guan, X.M., Yu, H., Trumbauer, M., Frazier, E., Van der Ploeg, L.H., and Chen, H. (1998). Induction of neuropeptide Y expression in dorsomedial hypothalamus of diet-induced obese mice. Neuroreport *9*, 3415–3419.

Guy, J., Hendrich, B., Holmes, M., Martin, J.E., and Bird, A. (2001). A mouse Mecp2-null mutation causes neurological symptoms that mimic Rett syndrome. Nat. Genet. *27*, 322–326.

Hagberg, B. (2002). Clinical manifestations and stages of Rett syndrome. Ment. Retard. Dev. Disabil. Res. Rev. *8*, 61–65.

Haskell-Luevano, C., and Monck, E.K. (2001). Agouti-related protein functions as an inverse agonist at a constitutively active brain melanocortin-4 receptor. Regul. Pept. *99*, 1–7.

Huszar, D., Lynch, C.A., Fairchild-Huntress, V., Dunmore, J.H., Fang, Q., Berkemeier, L.R., Gu, W., Kesterson, R.A., Boston, B.A., Cone, R.D., et al. (1997). Targeted disruption of the melanocortin-4 receptor results in obesity in mice. Cell *88*, 131–141.

Kesterson, R.A., Huszar, D., Lynch, C.A., Simerly, R.B., and Cone, R.D. (1997). Induction of neuropeptide Y gene expression in the dorsal medial hypothalamic nucleus in two models of the agouti obesity syndrome. Mol. Endocrinol. *11*, 630–637.

Kleefstra, T., Yntema, H.G., Oudakker, A.R., Romein, T., Sistermans, E., Nillessen, W., van Bokhoven, H., de Vries, B.B., and Hamel, B.C. (2002). De novo MECP2 frameshift mutation in a boy with moderate mental retardation, obesity and gynaecomastia. Clin. Genet. *61*, 359–362.

Klein, M.E., Lioy, D.T., Ma, L., Impey, S., Mandel, G., and Goodman, R.H. (2007). Homeostatic regulation of MeCP2 expression by a CREB-induced microRNA. Nat. Neurosci. *10*, 1513–1514.

Koizumi, H., Hashimoto, K., and Iyo, M. (2006). Dietary restriction changes behaviours in brain-derived neurotrophic factor heterozygous mice: role of serotonergic system. Eur. J. Neurosci. *24*, 2335–2344.

Kublaoui, B.M., Holder, J.L., Jr., Tolson, K.P., Gemelli, T., and Zinn, A.R. (2006). SIM1 overexpression partially rescues agouti yellow and diet-induced obesity by normalizing food intake. Endocrinology *147*, 4542–4549.

Lu, X.Y., Barsh, G.S., Akil, H., and Watson, S.J. (2003). Interaction between alpha-melanocyte-stimulating hormone and corticotropin-releasing hormone in the regulation of feeding and hypothalamo-pituitary-adrenal responses. J. Neurosci. *23*, 7863–7872.

Lubrano-Berthelier, C., Dubern, B., Lacorte, J.M., Picard, F., Shapiro, A., Zhang, S., Bertrais, S., Hercberg, S., Basdevant, A., Clement, K., and Vaisse, C. (2006). Melanocortin 4 receptor mutations in a large cohort of severely obese adults: prevalence, functional classification, genotype-phenotype relationship, and lack of association with binge eating. J. Clin. Endocrinol. Metab. *91*, 1811–1818.

Lyons, W.E., Mamounas, L.A., Ricaurte, G.A., Coppola, V., Reid, S.W., Bora, S.H., Wihler, C., Koliatsos, V.E., and Tessarollo, L. (1999). Brain-derived neurotrophic factor-deficient mice develop aggressiveness and hyperphagia in conjunction with brain serotonergic abnormalities. Proc. Natl. Acad. Sci. USA *96*, 15239–15244.

Martinowich, K., Hattori, D., Wu, H., Fouse, S., He, F., Hu, Y., Fan, G., and Sun, Y.E. (2003). DNA methylation-related chromatin remodeling in activity-dependent BDNF gene regulation. Science *302*, 890–893.

McGill, B.E., Bundle, S.F., Yaylaoglu, M.B., Carson, J.P., Thaller, C., and Zoghbi, H.Y. (2006). Enhanced anxiety and stress-induced corticosterone release are associated with increased Crh expression in a mouse model of Rett syndrome. Proc. Natl. Acad. Sci. USA *103*, 18267–18272.

Moretti, P., and Zoghbi, H.Y. (2006). MeCP2 dysfunction in Rett syndrome and related disorders. Curr. Opin. Genet. Dev. *16*, 276–281.

Moretti, P., Bouwknecht, J.A., Teague, R., Paylor, R., and Zoghbi, H.Y. (2005). Abnormalities of social interactions and home-cage behavior in a mouse model of Rett syndrome. Hum. Mol. Genet. *14*, 205–220.

Motil, K.J., Schultz, R.J., Browning, K., Trautwein, L., and Glaze, D.G. (1999). Oropharyngeal dysfunction and gastroesophageal dysmotility are present in girls and women with Rett syndrome. J. Pediatr. Gastroenterol. Nutr. *29*, 31–37.

Motil, K.J., Schultz, R.J., Abrams, S., Ellis, K.J., and Glaze, D.G. (2006). Fractional calcium absorption is increased in girls with Rett syndrome. J. Pediatr. Gastroenterol. Nutr. *42*, 419–426.

Mount, R.H., Charman, T., Hastings, R.P., Reilly, S., and Cass, H. (2002). The Rett Syndrome Behaviour Questionnaire (RSBQ): refining the behavioural phenotype of Rett syndrome. J. Child Psychol. Psychiatry *43*, 1099–1110.

Nicholson, J.R., Peter, J.C., Lecourt, A.C., Barde, Y.A., and Hofbauer, K.G. (2007). Melanocortin-4 receptor activation stimulates hypothalamic brain-derived neurotrophic factor release to regulate food intake, body temperature and cardiovascular function. J. Neuroendocrinol. *19*, 974–982.

Nuber, U.A., Kriaucionis, S., Roloff, T.C., Guy, J., Selfridge, J., Steinhoff, C., Schulz, R., Lipkowitz, B., Ropers, H.H., Holmes, M.C., and Bird, A. (2005). Up-regulation of glucocorticoid-regulated genes in a mouse model of Rett syndrome. Hum. Mol. Genet. *14*, 2247–2256.

Oswal, A., and Yeo, G.S. (2007). The leptin melanocortin pathway and the control of body weight: lessons from human and murine genetics. Obes. Rev. *8*, 293–306.

Rios, M., Fan, G., Fekete, C., Kelly, J., Bates, B., Kuehn, R., Lechan, R.M., and Jaenisch, R. (2001). Conditional deletion of brain-derived neurotrophic factor in the postnatal brain leads to obesity and hyperactivity. Mol. Endocrinol. *15*, 1748–1757.

Samaco, R.C., Fryer, J.D., Ren, J., Fyffe, S., Chao, H.T., Sun, Y., Greer, J.J., Zoghbi, H.Y., and Neul, J.L. (2008). A partial loss of function allele of methyl-CpG-binding protein predicts a human neurodevelopmental syndrome. Hum. Mol. Genet. *17*, 1718–1727.

Schwartz, M.W., Seeley, R.J., Woods, S.C., Weigle, D.S., Campfield, L.A., Burn, P., and Baskin, D.G. (1997). Leptin increases hypothalamic pro-opiomelanocortin mRNA expression in the rostral arcuate nucleus. Diabetes *46*, 2119–2123.

Shahbazian, M., Young, J., Yuva-Paylor, L., Spencer, C., Antalffy, B., Noebels, J., Armstrong, D., Paylor, R., and Zoghbi, H. (2002a). Mice with truncated MeCP2 recapitulate many Rett syndrome features and display hyperacetylation of histone H3. Neuron *35*, 243–254.

Shahbazian, M.D., Sun, Y., and Zoghbi, H.Y. (2002b). Balanced X chromosome inactivation patterns in the Rett syndrome brain. Am. J. Med. Genet. *111*, 164–168.

Spencer, C.M., Alekseyenko, O., Serysheva, E., Yuva-Paylor, L.A., and Paylor, R. (2005). Altered anxiety-related and social behaviors in the Fmr1 knockout mouse model of fragile X syndrome. Genes Brain Behav. *4*, 420–430.

Spencer, C.M., Serysheva, E., Yuva-Paylor, L.A., Oostra, B.A., Nelson, D.L., and Paylor, R. (2006). Exaggerated behavioral phenotypes in Fmr1/Fxr2 double knockout mice reveal a functional genetic interaction between Fragile X-related proteins. Hum. Mol. Genet. *15*, 1984–1994.

Stephens, T.W., Basinski, M., Bristow, P.K., Bue-Valleskey, J.M., Burgett, S.G., Craft, L., Hale, J., Hoffmann, J., Hsiung, H.M., Kriauciunas, A., et al. (1995). The role of neuropeptide Y in the antiobesity action of the obese gene product. Nature *377*, 530–532.

Takagi, N. (2001). The role of X-chromosome inactivation in the manifestation of Rett syndrome. Brain Dev. *23* (*Suppl 1*), S182–S185.

Tsao, D., Thomsen, H.K., Chou, J., Stratton, J., Hagen, M., Loo, C., Garcia, C., Sloane, D.L., Rosenthal, A., and Lin, J.C. (2008). TrkB agonists ameliorate obesity and associated metabolic conditions in mice. Endocrinology *149*, 1038–1048.

Unger, T.J., Calderon, G.A., Bradley, L.C., Sena-Esteves, M., and Rios, M. (2007). Selective deletion of Bdnf in the ventromedial and dorsomedial hypothalamus of adult mice results in hyperphagic behavior and obesity. J. Neurosci. *27*, 14265–14274.

Visel, A., Thaller, C., and Eichele, G. (2004). GenePaint.org: an atlas of gene expression patterns in the mouse embryo. Nucleic Acids Res. *32*, D552–D556.

Wade, J.M., Juneja, P., MacKay, A.W., Graham, J., Havel, P.J., Tecott, L.H., and Goulding, E.H. (2008). Synergistic impairment of glucose homeostasis in ob/ob mice lacking functional serotonin 2C receptors. Endocrinology *149*, 955–961.

Wang, C., Bomberg, E., Billington, C., Levine, A., and Kotz, C.M. (2007). Brain-derived neurotrophic factor in the hypothalamic paraventricular nucleus reduces energy intake. Am. J. Physiol. Regul. Integr. Comp. Physiol. *293*, R1003–R1012.

Weaving, L.S., Williamson, S.L., Bennetts, B., Davis, M., Ellaway, C.J., Leonard, H., Thong, M.K., Delatycki, M., Thompson, E.M., Laing, N., and Christodoulou, J. (2003). Effects of MECP2 mutation type, location and X-inactivation in modulating Rett syndrome phenotype. Am. J. Med. Genet. A. *118A*, 103–114.

Weaving, L.S., Ellaway, C.J., Gecz, J., and Christodoulou, J. (2005). Rett syndrome: clinical review and genetic update. J. Med. Genet. *42*, 1–7.

Williamson, S.L., and Christodoulou, J. (2006). Rett syndrome: new clinical and molecular insights. Eur. J. Hum. Genet. *14*, 896–903.

Xu, B., Goulding, E.H., Zang, K., Cepoi, D., Cone, R.D., Jones, K.R., Tecott, L.H., and Reichardt, L.F. (2003). Brain-derived neurotrophic factor regulates energy balance downstream of melanocortin-4 receptor. Nat. Neurosci. *6*, 736–742.

Yasui, D.H., Peddada, S., Bieda, M.C., Vallero, R.O., Hogart, A., Nagarajan, R.P., Thatcher, K.N., Farnham, P.J., and Lasalle, J.M. (2007). Integrated epigenomic analyses of neuronal MeCP2 reveal a role for long-range interaction with active genes. Proc. Natl. Acad. Sci. USA *104*, 19416–19421.

Yaylaoglu, M.B., Titmus, A., Visel, A., Alvarez-Bolado, G., Thaller, C., and Eichele, G. (2005). Comprehensive expression atlas of fibroblast growth factors and their receptors generated by a novel robotic in situ hybridization platform. Dev. Dyn. *234*, 371–386.

Young, D., Nagarajan, L., de Klerk, N., Jacoby, P., Ellaway, C., and Leonard, H. (2007). Sleep problems in Rett syndrome. Brain Dev. *29*, 609–616.

Zappella, M., Meloni, I., Longo, I., Hayek, G., and Renieri, A. (2001). Preserved speech variants of the Rett syndrome: molecular and clinical analysis. Am. J. Med. Genet. *104*, 14–22.

Zhou, Z., Hong, E.J., Cohen, S., Zhao, W.N., Ho, H.Y., Schmidt, L., Chen, W.G., Lin, Y., Savner, E., Griffith, E.C., et al. (2006). Brain-specific phosphorylation of MeCP2 regulates activity-dependent Bdnf transcription, dendritic growth, and spine maturation. Neuron *52*, 255–269.

Zoghbi, H.Y. (2005). MeCP2 dysfunction in humans and mice. J. Child Neurol. *20*, 736–740.